

# An Atlas<sup>\*</sup> of high resolution synthetic spectra in the wavelength region 4850 – 5400 Å

M. Chavez<sup>1</sup>, M.L. Malagnini<sup>2</sup>, and C. Morossi<sup>3</sup>

<sup>1</sup> Instituto Nacional de Astrofísica, Óptica y Electrónica INAOE. Apdos Postales 51 y 216, CP 72000 Puebla, Mexico

<sup>2</sup> Dipartimento di Astronomia, Università degli Studi di Trieste, Via G.B. Tiepolo, 11, I-34131 Trieste, Italy

<sup>3</sup> Osservatorio Astronomico di Trieste, Via G.B. Tiepolo, 11, I-34131 Trieste, Italy

Received November 26, 1996; accepted March 5, 1997

**Abstract.** We present an Atlas of high resolution (resolving power  $\lambda/\Delta\lambda = 250\,000$ ) synthetic spectra based on the 1993 release of atmosphere models and codes by Kurucz. The spectra are given in the wavelength interval 4850 – 5400 Å for eleven values of effective temperature in the range 4000 – 8000 K, for nine surface gravities in the interval 1.0 – 5.0 dex, and for seven metallicities spanning from –1.0 to +0.5 dex. The Atlas is aimed mainly at the analysis of composite stellar populations by means of suitable spectral features extracted from the spectra and identifiable in the observed composite light of clusters and galaxies. The high resolution used in the computations makes the Atlas also suitable for chemical abundance analyses.

**Key words:** stars: atmospheres — stars: late-type

## 1. Introduction

A comprehensive spectroscopic stellar library at high resolution provides a valuable tool for facing fundamental problems in different branches of astronomy. For instance, it can be used for determining the atmospheric parameters of stars by comparison with observed spectra (Cayrel et al. 1991a, b). On the other hand, synthetic spectra have proved to be an important (and sometimes the only) brick for the investigation of the behavior of prominent spectral features in terms of the stellar atmospheric parameters (e.g., Jones et al. 1996). Once this behavior has been properly modelled in stars, we can, in principle, predict the spectroscopic properties of stellar aggregates (e.g., Proc. of the conference “From Stars To Galaxies:

The Impact Of Stellar Physics On Galaxy Evolution”, Leitherer et al. 1996).

Out of the several aspects connected with the understanding of the evolutionary histories of stellar aggregates, we are particularly involved in the analysis and synthesis of spectral features typical of old stellar populations.

Along this line, we have computed a set of synthetic spectra in the wavelength interval 4850 – 5400 Å. This spectral region has been chosen because it contains conspicuous features, such as the Mg<sub>b</sub> triplet, the MgH molecular bands and FeI absorptions, which are easily observable in the integrated spectra of distant stellar systems. Moreover, the sensitivity of these lines to variations in surface gravity, effective temperature and metal content allows the determination of these parameters for individual stars in a self-consistent way.

We have not extended this region to include the blue wing of H<sub>β</sub> because of the poor fit between the observed and theoretical solar fluxes (Gulati 1989): the theoretical continuum appears too high with respect to the observed one.

Several reasons have been suggested to explain the discrepancy, among them problems in the convection treatment in the models or some underestimation of the continuum opacity (see, for instance, Castelli et al. 1997).

The spectra, computed with the upgraded versions of Kurucz’s models and codes (Kurucz 1993a-c), and based on revised atomic and molecular data, cover a parameter space suitable for the study of F, G and K stars, which are the dominant components in old stellar systems.

So far, these spectra have been already used for synthesizing a set of spectral features for population studies of clusters and galaxies observed at low and moderate resolution (Chavez et al. 1995, 1996). Since this application does not exhaust the informational content of the synthetic spectra, we are making available to the community the original high resolution spectra.

*Send offprint requests to:* M.L. Malagnini

\* Spectra are only available in electronic form at the CDS via anonymous ftp to cdsarc.u-strasbg.fr (130.79.128.5) or via <http://cdsweb.u-strasbg.fr/Abstract.html>

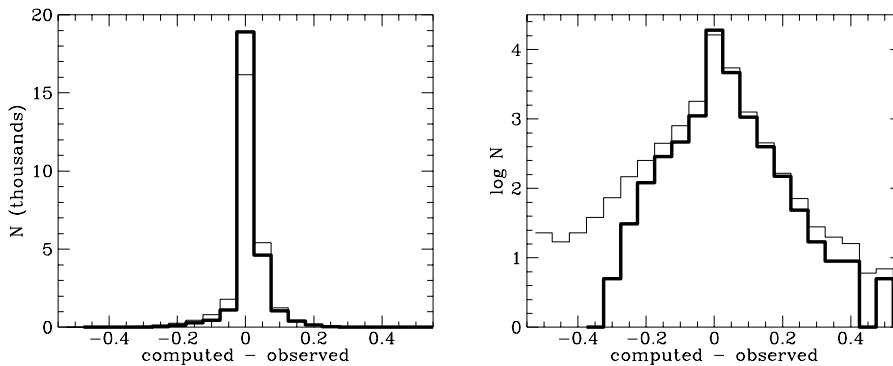


**Fig. 1. a and b)** Histogram of the residuals (computed – observed) for the synthetic spectra computed before (thin line) and after (thick line) adjusting the line parameters: **a)** the distribution in absolute numbers evidences the enhancement of the central bin, **b)** the logarithmic scale enhances the differences in the wings of the distribution

This paper describes the main characteristics and the format of the Atlas which can be obtained from the authors.

In Sect. 2 we present a short description of the line data used in the computations. Section 3 is devoted to present the characteristics of the spectra included in the Atlas. In Sect. 4 a subsample of the Atlas is presented in pictorial form suitable to highlight low resolution features.

## 2. The input line data

It is well known that the completeness and the accuracy of the atomic and molecular line data are of paramount importance for the reliability of any synthetic spectrum (see, for instance, Bell et al. 1994 and Kurucz 1995). To improve the reliability of the parameters governing the strength and the shape of the spectral lines, we compared the observed solar spectrum (Kurucz 1991) with a synthetic one. Empirical adjustments to line data were determined by applying a trial and error procedure as in Peterson et al. (1993). Our corrections, although small with respect to the uncertainties attributed to the line data parameters (Kurucz 1995), significantly improved the ability of the synthetic spectrum to mimic the observed one.

The model used for the comparison has the following atmospheric parameters:  $T_{\text{eff}} = 5777$  K,  $\log g = 4.43770$ , and element abundance from Anders & Grevesse (1989). For the micro- and macro turbulent velocities, the values 1 and  $1.5 \text{ km s}^{-1}$ , respectively, were adopted from Thévenin (1989). The synthetic spectrum was computed at the spectral resolution of  $\lambda/\Delta\lambda = 522\,000$ , so as to match the resolution of the observed spectrum.

The atomic and molecular line data were extracted from the updated line list compiled by Kurucz. The working line list includes more than 45 000 lines in the 4850 – 5400 Å spectral interval. Molecular features included in the computations are CN, C<sub>2</sub>, MgH, SiH and CH and account for the majority of the lines. Out of the working line list, about 1 500 lines were carefully investigated

and about 2000 modifications on their parameters ( $\log gf$  values and van der Waals damping constants) were applied. The improvement achieved after the modifications is testified by the decrease in the rms of the differences between the computed and the observed spectra (both normalized to the continuum and rebinned to the constant step  $\Delta\lambda = 0.02$  Å): by using the original line list, the rms value was 0.071 while is 0.049 after our modifications.

The distribution of the residuals (computed – observed residual intensities) is represented in Figs. 1a and b: the distribution obtained after the corrections clearly shows an higher concentration in the central bin (Fig. 1a: 18 903 instead of 16 157 data points over a total of 27 252). Figure 1b shows that the negative wing of the distribution is significantly reduced due to the removal of strong predicted lines which do not correspond to observed features; unfortunately, the improvement in the positive wing is less significant due to the impossibility of solving the problem of unidentified lines (see, for instance, the line at  $\sim 5170.8$  Å in Fig. 2).

Figures 2 and 3 illustrate in more detail the kind of modifications we performed by showing the region around a strong magnesium feature at 5172.684 Å and that one containing the iron feature at 5328.038 Å, respectively. In both figures, the thick solid line corresponds to the observed solar central intensity spectrum, the dotted line indicates the synthetic spectrum computed without modifying the line parameters and the thin solid line shows the spectrum computed after the modifications. The better agreement with the observations is the result of modifying the van der Waals damping constants and/or the  $\log gf$  values in the line data of Kurucz (1993b). Moreover, for some lines, small adjustments in wavelength were also required (see Fig. 3). For example, in order to match the observed profile with the theoretical one, the  $\gamma_{\text{VW}}$  of the central MgI line in Fig. 2 was corrected by subtracting 0.18 from the original value of  $-7.12$ . For the case of the iron feature at 5328 Å (Fig. 3), its  $\gamma_{\text{VW}}$  in Kurucz’s list ( $-7.87$ ) was increased by  $+0.30$ .

With the updated line list we computed the grid of high resolution synthetic spectra described in the next section.

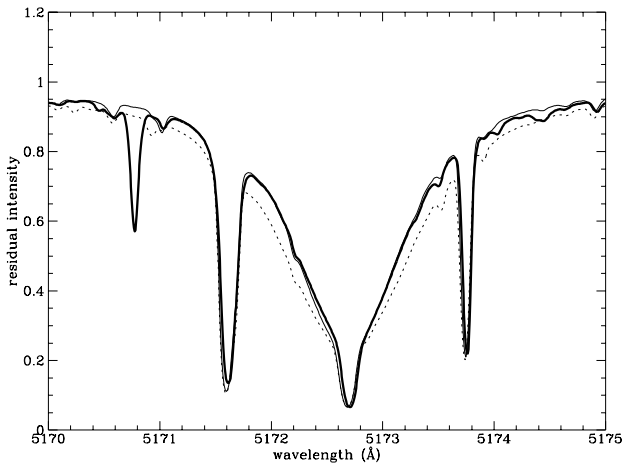


**Fig. 2.** Magnesium feature in the interval 5171 – 5174 Å. The thick solid line corresponds to the observed spectrum and the thin solid and dotted lines indicate the theoretical solar intensity spectra computed with and without adjusting the line parameters, respectively

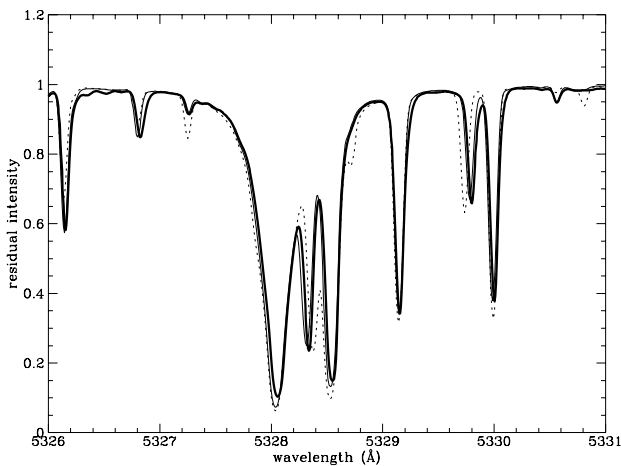


**Fig. 3.** Iron and Chromium features in the region 5327 – 5331 Å (symbols as in Fig. 2)

### 3. The synthetic spectra

Kurucz (1993a) model atmospheres are available in a range of temperatures that spans from 3 500 to 50 000 K, metallicities,  $[M/H]$ , from  $-3.5$  to  $+1.0$  and surface gravities ( $\log g$ ) from 0.0 to 5.0 dex. They have been computed by adopting a microturbulent velocity  $\xi = 2 \text{ km s}^{-1}$ . For the case of solar metallicity,  $[M/H] = 0.0$ , models

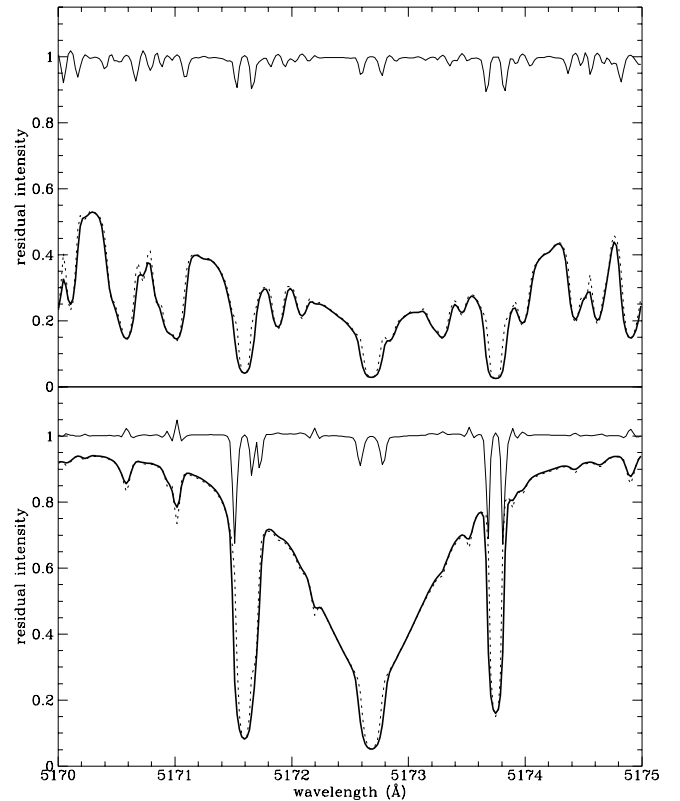


**Fig. 4.** Effects of microturbulent velocity in the Mg *b* region: spectra computed for  $\log g = 4.0$ ,  $[M/H] = +0.0$  and  $T_{\text{eff}} = 4000 \text{ K}$  (top),  $T_{\text{eff}} = 5500 \text{ K}$  (bottom). The thick solid line corresponds to  $\xi = 2.0 \text{ km/s}$  and the dotted line to  $\xi = 1.0 \text{ km/s}$ . The differences between the two spectra (thin solid line) are also plotted (a constant value equal to 1 was added for graphical reasons)

for different microturbulent velocities ranging from 0 to  $8 \text{ km s}^{-1}$  are also available (Kurucz 1993c).

For our purposes, models in the following ranges of parameters have been selected:

- Effective temperature from 4000 to 6000 K at a step of 250 K plus the spectra for 7000 and 8000 K;
- Surface gravity from 1.0 to 5.0 dex at a step of 0.5 dex;
- Overall chemical composition  $[M/H] = -1.0, -0.5, 0.0, 0.1, 0.2, 0.3, \text{ and } 0.5$ .

The fine steps in metallicity for  $[M/H] \geq 0.0$  make this grid more suitable for the analysis of the so-called super-metal rich stars than our previous theoretical grids (Gulati et al. 1993; Chavez et al. 1995). It must be noted that, in modelling stars with chemical composition different from solar, all heavy elements vary lock-step. Work is already planned in order to complement the Atlas by including synthetic spectra with non solar partitions in the  $\alpha$ -elements once the appropriate models are available.

All the 693 spectra have been computed at the resolving power  $\lambda/\Delta\lambda = 250\,000$ , rotational velocity of  $0 \text{ km s}^{-1}$  and microturbulent velocity  $\xi = 2 \text{ km s}^{-1}$ .

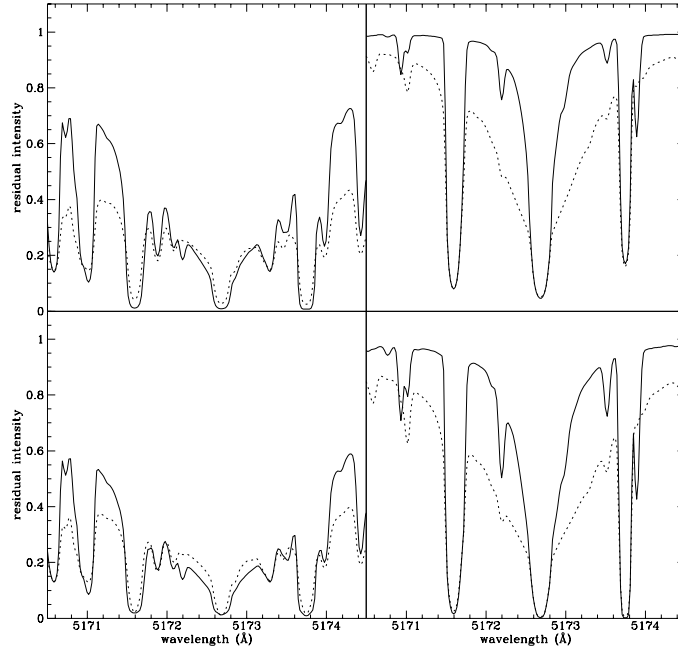


**Fig. 5.** Effects of different atmosphere parameter values in the Mg *b* region: spectra computed for  $T_{\text{eff}} = 4000$  K (left) and  $T_{\text{eff}} = 5500$  K (right) at  $[M/H] = +0.0$  (top) and  $[M/H] = +0.5$  (bottom) are plotted. The solid line corresponds to  $\log g = 1.5$ , and the dotted line to  $\log g = 4.0$

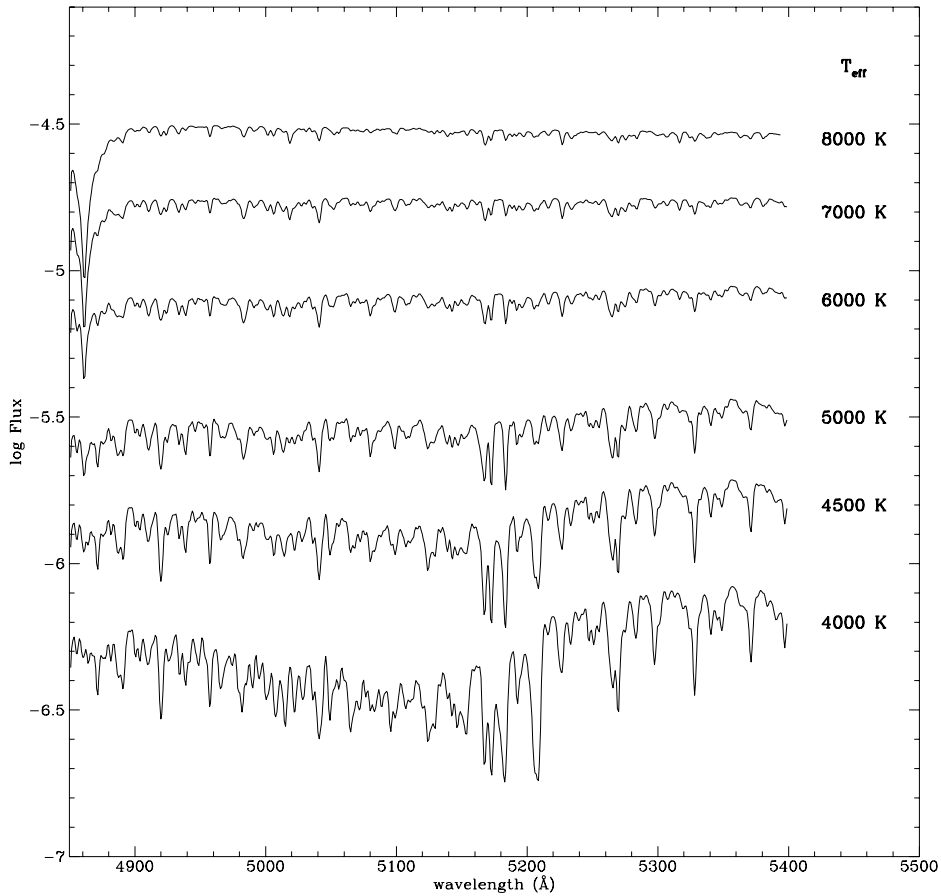


**Fig. 6.** Sequence in temperature of spectra representative of solar chemical composition stars of intermediate surface gravity ( $\log g = 3.0$  dex)

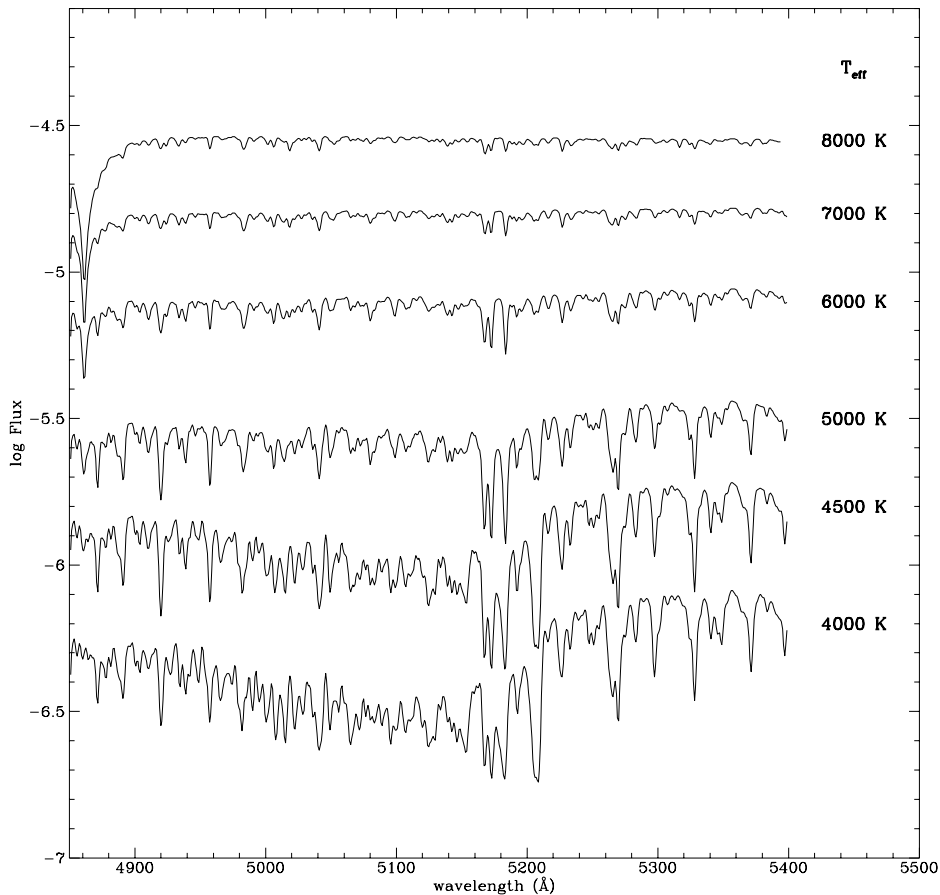


**Fig. 7.** Sequence in temperature of spectra representative of solar chemical composition dwarfs ( $\log g = 4.5$  dex)

The use of a fixed value for  $\xi$  is somewhat arbitrary (see Kurucz 1996 for a detailed discussion). Among synthetic spectra builders, different approaches have been followed. For instance, Barbuy (1994) considers a value of  $\xi = 1.0 \text{ km s}^{-1}$  for stars with gravities  $\log g \geq 2.0$ , and  $\xi = 1.8 \text{ km s}^{-1}$  for stars with  $\log g < 2.0$ , and Milone et al. (1995) adopt  $\xi = 1.0 \text{ km s}^{-1}$  for  $\log g \geq 3.5$ ,  $\xi = 1.5 \text{ km s}^{-1}$  for giant stars with  $2.0 \leq \log g \leq 3.0$ , and  $2.0 \text{ km s}^{-1}$  for supergiants ( $\log g \leq 1.5$ ). Tripicco & Bell (1995) have smoothly varied the value of  $\xi$  from  $1.0 \text{ km s}^{-1}$  for dwarf stars to  $2.0 \text{ km s}^{-1}$  for supergiants.

At present Kurucz’s models for other microturbulent velocities are available only for solar chemical abundance. In order to get insight into the effects of this parameter we have computed an additional set of 18 synthetic spectra with the following parameters: surface gravity fixed at  $\log g = 4.0$ , temperatures ranging from 3500 to 8000 K with a step of 500 K, and microturbulent velocities  $\xi = 0.0 \text{ km s}^{-1}$  and  $\xi = 1.0 \text{ km s}^{-1}$ . The effects of different  $\xi$ ’s on spectral indices have been discussed in Chavez et al. (1996): in general, they are negligible at high temperatures, while becoming of some significance at low temperatures. At high resolution, the microturbulent velocity effects are temperature and wavelength dependent. As

an example, Fig. 4 shows the synthetic spectra computed with different microturbulent velocities ( $\xi = 1.0 \text{ km s}^{-1}$  and  $\xi = 2.0 \text{ km s}^{-1}$ ) for two temperatures, namely 4000 K and 5500 K, in the wavelength region dominated by the Mg *b* triplet. In both panels, the differences between the two spectra are also plotted. The average flux difference is larger for 4000 K, while, locally, the differences are higher for 5500 K.

#### 4. The Atlas

The Atlas consists of 711 sets of data. Each set contains a description which specifies the main spectrum parameters, i.e. temperature, surface gravity, chemical composition and microturbulence of the parent model, wavelength range, resolving power, etc. Then, for each wavelength point, both the continuum and the line blanketed absolute fluxes per unit frequency ( $\text{erg cm}^{-2} \text{ s}^{-1} \text{ Hz}^{-1}$ ) are given allowing the computation of residual intensities. The Atlas is published electronically at the CDS.

A subset of the spectral Atlas is displayed in Figs. 5, 6 and 7. Figure 5 illustrates the behaviour of the spectra in the Mg *b* region for different temperatures, metallicities, and surface gravities.

The general trend of the spectra in the whole wavelength range is depicted in Figs. 6 and 7. The spectra are plotted in an absolute flux scale after a degradation in resolution ( $FWHM = 2.5 \text{ \AA}$ ) to increase the readability of the figures. Figures 6 and 7 contain sequences in temperatures of spectra representative of solar chemical composition stars of intermediate and high surface gravity, 3.0 dex and 4.5 dex, respectively.

Figures 5 to 7 show that our Atlas can serve as a starting point both for high and for intermediate resolution analyses. In fact, the availability of synthetic spectra at high resolution makes it possible to simulate the effects of any instrumental profile.

*Acknowledgements.* This work was partially supported by the Ministero dell'Università e della Ricerca Scientifica e Tecnologica (60% and 40% grants), and by the Consiglio Nazionale delle Ricerche (CNR–GNA).

## References

- Anders E., Grevesse N., 1989, *Geochim. Cosmochim. Acta* 53, 197
- Barbuy B., 1994, *ApJ* 430, 218
- Bell R.A., Paltoglou G., Tripicco M.J., 1994, *MNRAS* 268, 771
- Castelli F., Gratton R.G., Kurucz R.L., 1997, *A&A* 318, 841
- Cayrel R., Perrin M.-N., Barbuy B., Buser R., 1991a, *A&A* 247, 108
- Cayrel R., Perrin M.-N., Buser R., Barbuy B., Coupry M.-F., 1991b, *A&A* 247, 122
- Chavez M., Malagnini M.L., Morossi C., 1995, *ApJ* 440, 210
- Chavez M., Malagnini M.L., Morossi C., 1996, *ApJ* 471, 726
- Gulati R.K., 1989, M. Phil. thesis, SISSA
- Gulati R.K., Malagnini M.L., Morossi C., 1993, *ApJ* 413, 166
- Jones J.B., Gilmore G., Wyse R.F.G., 1996, *MNRAS* 278, 146
- Kurucz R.L., 1991, *Rev. Mexicana Astron. Astrofis.* 23, 187
- Kurucz R.L., 1993a, CD–Rom 13, ATLAS9 Stellar Atmospheres Programs and 2 km/s Grid. Cambridge: Smithsonian Astrophys. Obs.
- Kurucz R.L., 1993b, CD–Rom 18, SYNTHE Spectrum Synthesis Programs and line data. Cambridge: Smithsonian Astrophys. Obs.
- Kurucz R.L., 1993c, CD–Rom 19, Solar Abundance Model Atmospheres for 0, 1, 2, 4, 8 km/s. Cambridge: Smithsonian Astrophys. Obs.
- Kurucz R.L., 1995, “Rapid Calculation of Line Opacity”, CfA preprint No. 4080, to appear in *Computational Astrophysics*, Vol. 2, Stellar Physics, Kudritzki R. et al. (eds.)
- Kurucz R.L., 1996, “Model Stellar Atmospheres and Real Stellar Atmospheres”, CfA preprint No. 4372, ASP Conf. Ser. 108, Adelman S.J., Kupka F., and Weiss W.W. (eds.) (in press)
- Leitherer C., Fritze–von Alvensleben U., Huchra J., 1996, ASP Conf. Ser. 98
- Milone A., Barbuy B., Bica E., 1995, *A&AS* 113, 547
- Peterson R., Dalle Ore C.M., Kurucz R.L., 1993, *ApJ* 404, 333
- Thévenin F., 1989, *A&AS* 77, 137
- Tripicco M.J., Bell R.A., 1995, *AJ* 110, 3035